ELSEVIER

Journal of Nuclear Materials 318 (2003) 325–332

journal of nuclear materials

www.elsevier.com/locate/jnucmat

Corrosion behaviour of steels and refractory metals and tensile features of steels exposed to flowing PbBi in the LECOR loop

C. Fazio [a,*], I. Ricapito [b], G. Scaddozzo [c], G. Benamati [a]

[a] *ENEA – CR Brasimone, I – 40032 Camugnano Bologna, Italy*
[b] *ESA s.a.s, I – 40033 Casalecchio di Reno, Bologna, Italy*
[c] *Politecnico di Torino, Corso Duca degli Abruzzi 24, I – 10129 Torino, Italy*

Abstract

An experimental activity has been started using the LECOR loop at the ENEA Brasimone centre to investigate the corrosion behaviour of steels and refractory metals as well as the tensile properties of steels exposed to flowing liquid lead bismuth with low oxygen activity. The oxygen content in the liquid metal was controlled and monitored by a dedicated system. The compatibility test was performed at 673 K and the corrosion and tensile results herein reported concern the first 1500-h run of the loop operation. All the materials tested suffered from liquid metal attack exhibiting a weight loss. The consequent evaluation of the corrosion rate showed that, under the given test conditions, the refractory metals are more resistant than the steels. The tensile properties of austenitic steel are not affected by the liquid metal corrosion, while the martensitic steel exhibited a mixed brittle–ductile fracture surface.

1. Introduction

Liquid lead or eutectic lead–bismuth have been proposed both as spallation target and as coolant in accelerator driven systems (ADS), which aim to burn radioactive waste from conventional nuclear power plants. As has been well described in the past [1,2] the ADS consists of proton beam impinging a liquid metal target and a subcritical core. Neutrons are produced by the proton beam striking the liquid metal target, thereby inducing a spallation reaction. A design of a Demonstrator (DEMO) reactor has been produced by the Italian company named ANSALDO [2] and a large R & D programme is ongoing within the European Union to demonstrate the feasibility of ADS. Within the R & D programme the international project MEGAwatt Pilot target Experiment (MEGAPIE) in Switzerland [3] and the MYRRHA project, which consists in the development of a Multipurpose Neutron Source for R & D Applications on the basis of an ADS, in Belgium [4] have the aim of demonstrating the operability of such liquid metal targets. Both of these initiatives have planned to use liquid eutectic lead–bismuth, which satisfies the requirements for neutron production and also because it possesses suitable physical properties, i.e. low melting point and low vapour pressure. However, it is well known that materials compatibility issues should be considered when using liquid metal. Indeed, it has already been comprehensively reported that the mechanism and rate of the corrosion of structural materials when exposed to liquid lead or eutectic lead–bismuth, at the operation temperature of the target, are strongly dependent upon the oxygen activity in the liquid metal [5,6]. For instance, it has been demonstrated that for a sufficiently high oxygen activity in heavy liquid metals, oxide layers are developed both on steels [7] and on refractory metals [8,9]. Although during the 1960s, some corrosion tests were performed on low-alloy steel exposed to deoxidised heavy liquid metal [10], a complete

* Corresponding author. Tel.: +39-0534 801463; fax: +39-0534 801225.
E-mail address: concetta.fazio@psf.fzk.de (C. Fazio).

0022-3115/03/$ - see front matter
doi:10.1016/S0022-3115(03)00009-6

perspective on the corrosion behaviour under the proposed operation conditions cannot be drawn from the existing literature. The aim of the experimental activities here presented is to describe the corrosion mechanism and to estimate the corrosion rate of selected materials exposed to flowing Pb–Bi with a low oxygen activity. The experiments were performed in the LECOR (LEad CORrosion) loop designed and constructed at the ENEA site of Brasimone. The loop testing parameters were chosen to be as similar as possible to the experimental conditions of the MEGAPIE target and also, to some extent, to the MYRRHA target. A detailed description of the loop, as well as the oxygen control system employed will be presented. The materials analysed were austenitic steel, martensitic steel and refractory metals. In addition to the identification of the corrosion process, tensile properties of the steels after exposure to the liquid metal were also tested. The experimental programme of LECOR is planned to extract samples from the test section every 1500 h, up to a maximum of 4500 h. The results here presented refer to analyses performed on the materials corroded for 1500 h.

2. Experimental

2.1. LECOR plant

According to Fig. 1, the LECOR plant has a 'figure-of-eight' configuration, typical for a corrosion loop, with a high temperature branch running from the economiser (EX) to the test sections (TS) and a low temperature branch including the delivery and return pipes between the S2 tank and the economiser, including the by-pass line. The S2 vessel contains a mechanical pump, with submerged impeller, sized to provide the loop with a maximum liquid metal flow rate of 4 m^3/h corresponding to a velocity in the test sections of 3 m/s.

The three test sections (TS1/2/3) containing the specimens to be investigated are placed downstream of the electrical heater (H). The samples are piled up in the test section and separated from each other with spacers. In the steady state, the thermal power provided by the heater is equal to that extracted by the forced air heat exchanger (C). The electrical heater (H) can supply a maximum power of 82 kW, and is operated by a PID thermal regulator connected to a socket thermocouple located at the exit, with H and C responsible for the ΔT between the hot and cold branches. This configuration enables a continuous transport of corrosion products from the hot region, where the test sections are located, to the cold region where they are partially released, simulating the actual behaviour of coolant fluid in a thermal production plant. The total liquid metal flow rate available to the test sections is adjusted through the by-pass line, whilst the liquid metal flow rate in each test section is automatically controlled by electro-pneumatic regulation valves driven by feedback signals from electromagnetic flowmeters (EF).

To carry out the experimental campaign with well-defined oxygen content in the liquid metal, an oxygen electrochemical sensor (Ox) is placed in the hot region, close to one of the test sections. Moreover, the vessel S1, which acts as drain and storage tank, is connected to an external gas system that allows the oxygen content in the liquid metal to be reduced by injection of Ar/H_2 mixture.

The structural materials of the loop are as follows: the cold part is fabricated in austenitic steel (AISI 316L), while the hot region is in ferritic steel (Cr–Mo Steel) representing a good compromise between the require-

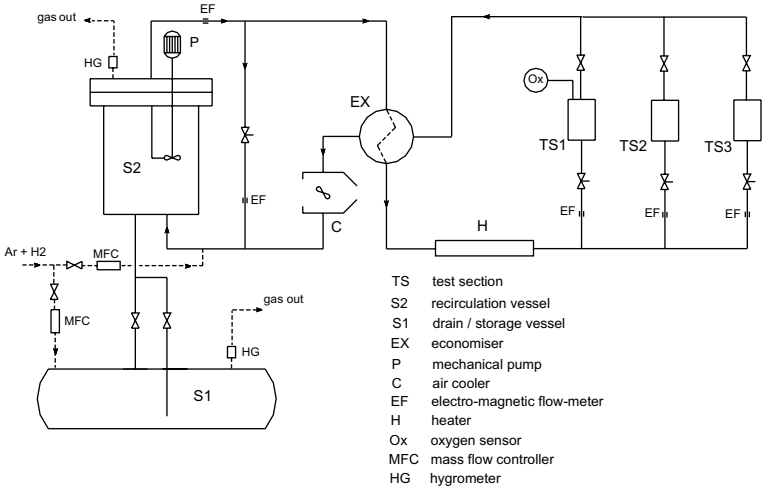

Fig. 1. Scheme of the LECOR loop.

Table 1
Main characteristics of the LECOR loop

Pb–Bi inventory (m^3)	0.6
Maximum Pb–Bi flow rate in the pump delivery line (m^3/h)	4
Maximum temperature in the test section (°C)	550
Total installed electrical power (kW)	150
Maximum heating power of the heater H (kW)	82
Maximum heat exchange power in EX (kW)	240
Design pressure (barg)	4

ments of acceptable ductility and corrosion resistance in a liquid metal environment.

Loop operation is automatically controlled by a PLC, connected to a supervisor PC that also runs the data acquisition software. Characteristics of the main LECOR components are given in Table 1.

2.2. Oxygen control and monitoring system

To perform the corrosion tests in the LECOR loop using liquid metal with a low oxygen activity, 80 wppm of pure Mg were added to the eutectic lead–bismuth. In addition, pre-treatment with hydrogen gas was performed in the storage tank for a few days at 603 K. The aim of adding Mg was to deoxidise the liquid metal, since Mg forms much more stable oxides than Pb and Bi [11]. The hydrogen pre-treatment was performed taking advantage of the oxide reduction kinetic studies previously performed [12], and monitored by evaluating the water extraction rate from the drain tank. During circulation of the liquid metal, the oxygen activity was measured with an oxygen sensor placed in the hot part of the loop. This oxygen sensor, constructed at the IPPE of Obninsk, has the red-ox pair Bi/Bi_2O_3 as reference electrode and Ytrria stabilised zirconia acting as a solid electrolyte. The probe had been previously calibrated in the Russian laboratories and was delivered to ENEA with the calibration equation [22]. During the 1500-h run of the LECOR loop, the electromotive force readings of the probe were recorded by a data acquisition system, and those data and the corresponding oxygen activity are reported in Fig. 2, where oxygen activity was calculated using the calibration equation. As can be seen in that diagram, the measured oxygen activity was between 2.3×10^{-6} and 5.5×10^{-4}, corresponding to 3.1×10^{-10} and 7.3×10^{-8} wt% of oxygen dissolved in the liquid metal.

2.3. Materials, test parameters and post test analysis

Cylindrical machined corrosion specimens 10 mm in diameter and 50 mm in length, as well as cylindrical tensile specimens 3 mm in diameter and gauge length 10 mm were machined for the testing programme. The tested materials were AISI 316L and T91 steels and the refractory metals tungsten and molybdenum. The two steels were tested for both corrosion and tensile performance, whilst only the corrosion behaviour of the two refractory metals was tested. The W and Mo, supplied by Elettroleghe s.r.l of Italy, were fabricated by sintering and had purities of 99.9 and 99.95 wt% respectively, while the composition of the two steels is reported in Ref. [7]. The lead–bismuth used in the loop, was supplied by Stachow of Germany, and was composed 44.8

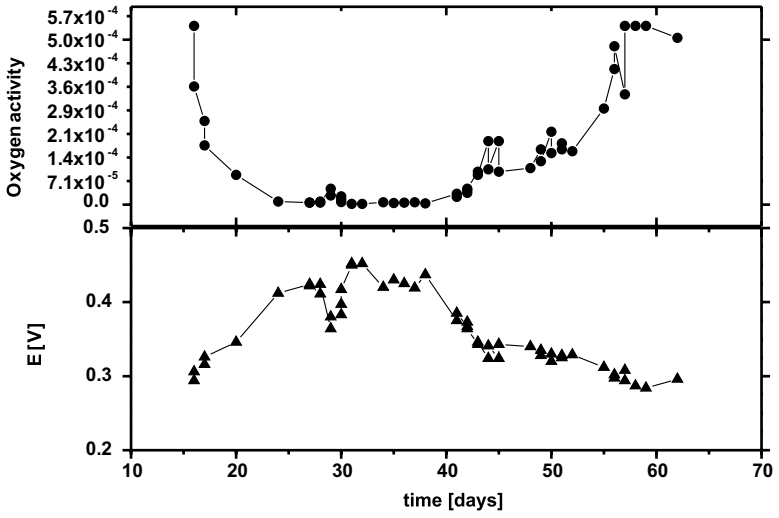

Fig. 2. Electromotive force and oxygen activity in the liquid metal recorded during the 1500 h run.

by wt% of Pb and 55.2 wt% of Bi with some minor impurities. The temperature in the test sections of the loop was 673 K and the cold part of the loop was at 573 K. The flow of liquid metal around the samples was 120 l/h corresponding to a velocity of 1 m/s and the Reynolds number was about 1×10^4, indicating a turbulent flow. Every 1500 h of liquid metal circulation in the loop, a set of samples was extracted from the test sections, where two corrosion samples for each type of material and four tensile samples for each type of steel were taken. In order to extract the samples from the test sections the loop is drained and cooled down, the flanged test sections are opened and the specimens were extracted. After extracting the samples from the test section, the corrosion rates of the four materials were evaluated by means of the weight change measurement technique. For each material, one of the corrosion samples was cleaned with a solution made by CH_3COOH, H_2O_2, C_2H_5OH in a ratio of 1:1:1, with the cleaning procedure performed until the weight of the specimen remained constant. Each second corrosion specimen was cut, mounted, lapped and etched in order to perform metallurgical analyses on its cross section with the aid of an optical microscope and scanning electron microscope (SEM). The chemical compositions of the corroded layers were evaluated by means of energy dispersive X-ray spectroscopy (EDX) using ZAF correction method. The ZAF correction method converts the X-ray intensities to concentration. It is based on measurement of the pure element intensities and composition of corrected factors for the 'atomic number effect', **Z**, the 'absorption correction', **A** and the 'fluorescence correction', **F**.

The sets of four tensile specimens were tested with the SYNTECH test machine at 673 K and under Ar atmosphere without removing the traces of Pb–Bi alloy from their surfaces. The tensile tests were conducted under strain-controlled conditions with an extension rate of 2 mm/min which corresponds to an initial strain rate of 3×10^{-3} s^{-1}.

3. Results and discussion

3.1. Steels

The weight change measurements performed on the samples after 1500 h of exposure to the liquid metal showed a weight loss for both steels. The corresponding evaluated corrosion rate is 1.52×10^{-5} mg/mm^2 h (1.9×10^{-3} μm/h) for the austenitic steel AISI 316L, and 2.47×10^{-5} mg/mm^2 h (2.9×10^{-3} μm/h) for the martensitic steel T91. Fig. 3 shows the SEM micrograph of the AISI 316L cross section. In order to reveal the microstructure of the corroded layer and the bulk, the cross section was etched with a solution of oxalic acid.

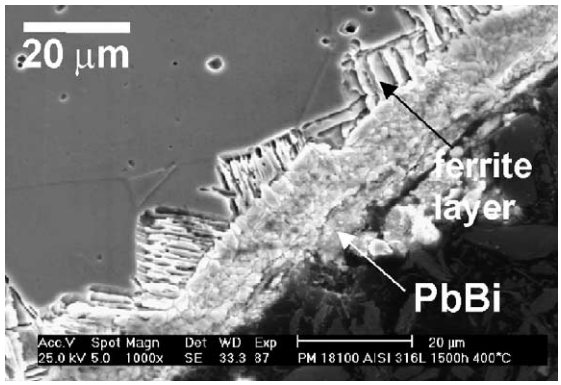

Fig. 3. SEM micrograph of the AISI 316L cross section etched with oxalic acid.

As it can be observed in Fig. 3 the surface of the steel underwent a liquid metal attack, developing a corroded porous layer with laminar morphology. The EDX analyses performed on this layer, but on a not etched part, showed a relevant Ni depletion and also the Cr content was less than in the bulk material. The electron probe micro analysis (EPMA) indicates that ferritisation had occurred, and it was also observed that the thickness of the ferrite layer was not uniform, ranging from few micrometer to about 14 μm. The observed ferritisation indicates that leaching of the steel elements in the liquid metal is a relevant parameter in the AISI 316L corrosion mechanism under the given test conditions. In fact the solubility of Ni, Cr and Fe in the eutectic Pb–Bi at 673 K is about 16000 wppm, 3.90 wppm and less than 1 wppm [6] respectively, considerably supporting the experimental results.

The appearance of the cross sections of the corroded sample of martensitic steel T91 is shown in the SEM micrographs of Figs. 4 and 5. In those figures, liquid metal penetration was visible as well as the presence of cavities at the surface of the steel. Considering the morphology of the steel–liquid metal interface, it appears that the corrosion proceeds via transgranular and intergranular dissolution of the steel elements. Further, a preferential dissolution of steel elements could not be observed, as was for instance reported for martensitic steel exposed to Pb–17Li [13,14] where Cr depleted corrosion layers were detected. Nevertheless, it should be taken into account that in these works the flow rate of the Pb–17Li was about 100 times lower than the flow rate of the Pb–Bi in LECOR. Thus, in assuming the same corrosion mechanism in Pb–17Li and in Pb–Bi, a flaking of the Cr depleted corrosion layer might occurred with the higher flow rate.

Literature data about the corrosion rate of steels in in Pb–Bi with low oxygen content is sparse [15], but literature data on the corrosion of steels in Pb–17Li is

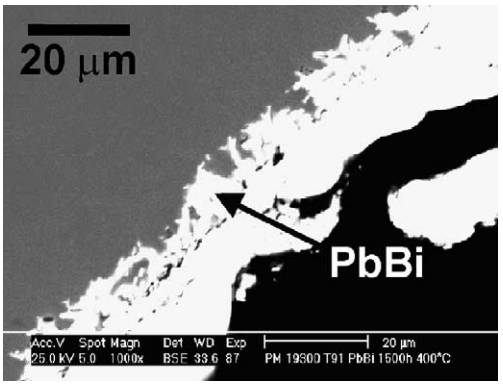

Fig. 4. SEM micrograph of the unetched T91 cross section.

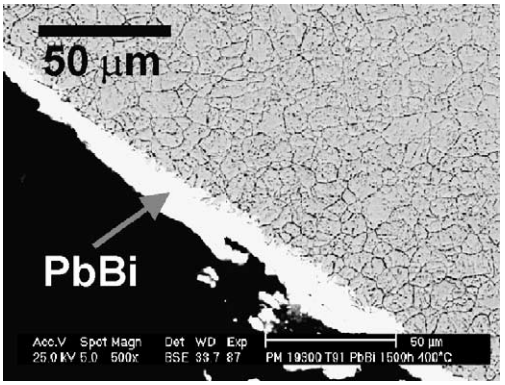

Fig. 5. SEM micrograph of the T91 cross section etched with oxalic acid.

plentiful [16]. Since the oxygen solubility at 673 K in Pb–17Li is about 10^{-8} wt% [24], the Pb–17Li environment is arguably similar to Pb–Bi from the low oxygen activity point of view, thus the Pb–17Li data can be considered useful. Both of these references report that austenitic steels exhibit a higher corrosion rate than martensitic steels. Thus, it appears that the comparable corrosion rates of the austenitic and martensitc steels here observed do not agree with the cited literature, although it could be assumed that the steel element dissolution was itself preceded by decomposition of the natural oxide layer present on the steel surfaces. A similar process has been described in the past to explain the observed corrosion rate data obtained in Pb–17Li, which exhibited a discontinuity with increasing exposure time [17,23]. Further measurements on specimens extracted from the LECOR loop after 3000 and 4500 h of exposition could help to confirm this assumption.

The results obtained from the tensile tests performed on the two types of steels before and after corrosion are reported in Table 2. Here the average values of the yield (R (0.2%)) and ultimate tensile strength (UTS) as well as elongation (A %) and area reduction (Z %) factors are given. In Fig. 6 a pair of stress–strain curves of AISI 316L steel corroded and non-corroded and in Fig. 7 a

Table 2
Tensile test results (mean values) obtained at 673 K on non-corroded and corroded AISI 316L and T91 steels

	UTS (MPa)	R (0.2%) (MPa)	A %	Z %
AISI 316 L				
As received	457 ± 40	165 ± 35	69 ± 3	73 ± 3
1500 h corr.	477 ± 9	183 ± 26	68 ± 3	72 ± 5
T91 steel				
As received	644 ± 26	532 ± 42	22 ± 1	72 ± 2
1500 h corr.	639 ± 14	522 ± 10	18 ± 1	42 ± 8

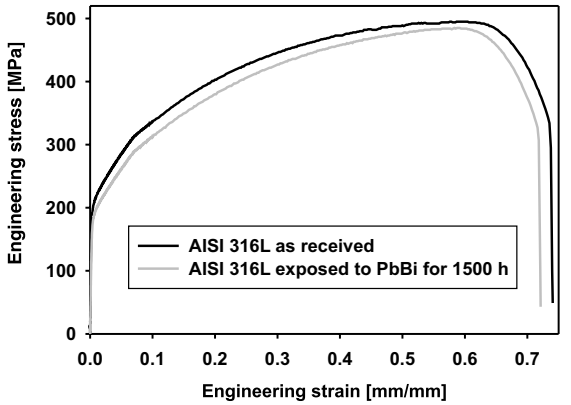

Fig. 6. Engineering tensile curves of the non-corroded (as received) and corroded AISI 316L samples.

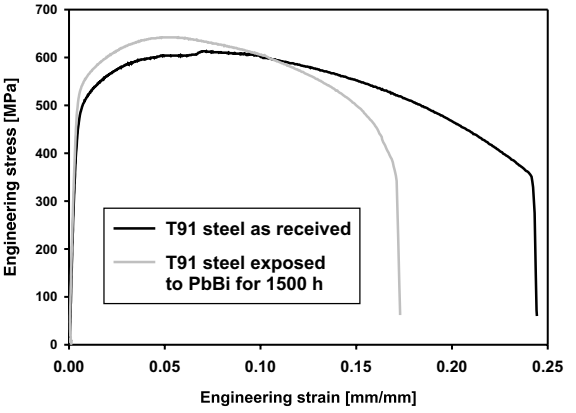

Fig. 7. Engineering tensile curves obtained on the non-corroded (as received) and corroded T91 samples.

pair of stress–strain curves of T91 specimens corroded and non-corroded are reported.

Comparing the tensile behaviour of the non-corroded and corroded austenitic steel it can be seen that the Pb–Bi corrosion and the consequent ferritisation did not affect its tensile behaviour (see Table 2 and the curves reported in Fig. 6). Conversely, the corroded martensitic steel produced a much lower area reduction factor (42%, see Table 2) with respect to the non-corroded specimens (72%, see Table 2). The metallographic analysis of the AISI 316L and T91 fracture surfaces are reported in the SEM micrographs of Figs. 8 and 9 respectively. As is shown in these figures, the bulk surface area of both steels shows a dimpled fracture, which is the typical morphology of ductile behaviour. Pb–Bi could be detected in the external part of both types of steel, indicating an intimate contact between the liquid metal and the steel. The main differences that were observed between the two steels was that on the periphery of the T91 fracture surface a flat morphology could be seen with the presence of microcracks, whilst on the AISI 316L steel the same morphology was not present. This behaviour of the corroded T91 steel is quite different to similar past work performed on martensitic steels exposed to Pb–17Li [13,18,19], where the liquid metal did not affect the tensile properties. Moreover, liquid metal embrittlement

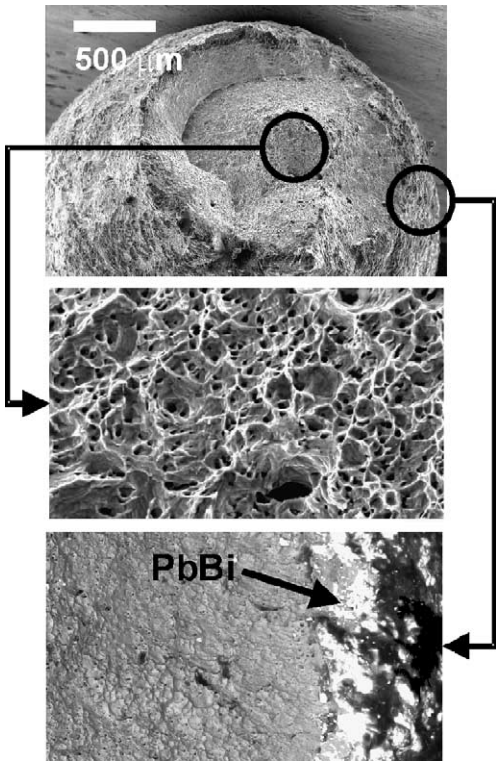

Fig. 8. SEM micrograph, fracture surface of the AISI 316L sample.

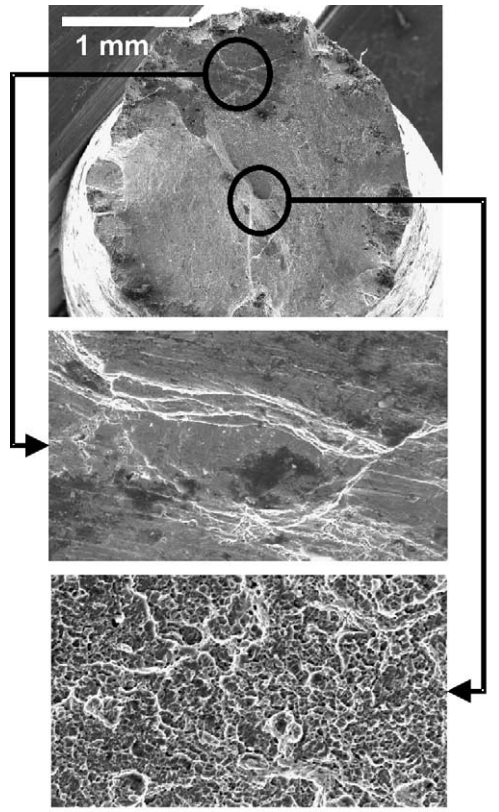

Fig. 9. SEM micrograph, fracture surface of the T91 sample.

tests performed in Pb [20] and Pb–17Li [21] have shown no influence on the mechanical behaviour of normal heat-treated martensitic steels.

It could be that the more aggressive Bi in the Pb–Bi alloy together with long exposure of the T91 steel to the liquid metal might play some role in the decrease of the area reduction coefficient observed. Tensile tests of the LECOR corroded samples after 3000 and 4500 h are expected to give a clearer idea of this phenomenon. It could be assumed that also low cycle fatigue tests might give more indications about the liquid metal effect on the mechanical performances of the steels.

3.2. Refractory metals

The measured weight loss of both the tungsten and molybdenum samples was 7.26×10^{-7} mg/mm^2 h (7.1×10^{-5} μm/h) and 9.1×10^{-7} mg/mm^2 h (4.7×10^{-5} μm/h) respectively. From a metallographic point of view, as is shown in the SEM micrograph of Figs. 10 and 11 both metals exhibited an almost smooth interface with the lead–bismuth alloy. No evidence of liquid metal attack on the surface of the two materials, or of the growth of an oxide layer, could be detected. The weight loss measured could be associated with both the uniform

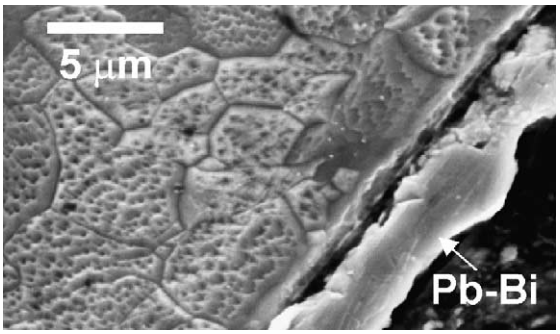

Fig. 10. SEM micrograph of the W cross section.

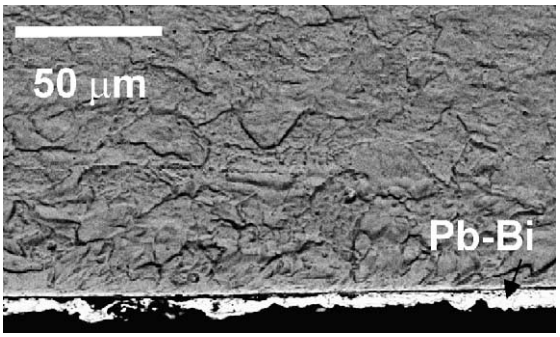

Fig. 11. SEM – micrograph of the Mo cross section.

dissolution and the low solubility of W and Mo in Pb–Bi liquid at 673 K. In comparing the estimated corrosion rate obtained on the refractory metals with that obtained on steels, it is evident that the low oxygen content in the liquid metal, the refractory metals exhibited two orders of magnitude greater resistance to corrosion than the steels. On the other hand, previous studies [8,9] performed in static and oxygen saturated lead at 793 K have shown that W and Mo exhibit friable and not protective oxides. Even though the test temperature in these studies is higher than the LECOR temperature, calculations of the free energy of oxides formation suggest that these would be likely even at 673 K, given sufficient oxygen activity in the liquid metal.

4. Conclusions

The aim of the LECOR loop is to perform materials compatibility tests in Pb–Bi eutectic having a low oxygen activity, thereby simulating the conditions of the structural materials of both the MEGAPIE and the MYRRHA targets. The low oxygen activity was achieved by adding Mg, which acts as oxygen getter, and by pre-conditioning the liquid metal with hydrogen gas. The oxygen activity was successfully monitored during the test with an oxygen probe installed on the hot part of the loop. All the materials tested in the LECOR loop exhibited a weight loss after 1500 h of exposure. The measured corrosion rate of W and Mo, in the range of 10^{-5} μm/h, was two order of magnitude lower than that of the AISI 316L and T91 steels. As regards the corrosion mechanism, the AISI 316L steel exhibited mainly a Ni depletion and consequent ferritisation to a maximum depth of 14 μm from the surface. The T91 steel underwent steel element dissolution with the formation of cavities and no depleted layer could be observed. Moreover, the estimated corrosion rates of the austentic steel and the martensitic steel were of the same order of magnitude, which can be explained assuming a first step of decomposition of the natural oxide layer usually present on the steels. Further ongoing experiments will confirm this assumption. The tensile behaviour of the AISI 316L seems to be unaffected by corrosion in flowing Pb–Bi, while the T91 steel exhibited a decrease of the area reduction factor with a mixed ductile–brittle fracture morphology. It was assumed that a relationship between the brittle fracture mode occurring mainly on the peripheral part of the T91 tensile samples, and the presence of Bi plus the long exposure time to the liquid metal could give rise to this phenomenon. More experiments will be needed to confirm this assumption.

Acknowledgements

This work has been supported by the EU project TECLA. The authors are grateful to Mr L. Rapezzi and his collaborators for operation of the LECOR loop, to Mr A. Agostini and his colleagues of the ENEA-Brasimone Laboratory of Metallurgy for the specimen preparation assistance and to Mr S. Storai for performing the tensile tests.

References

[1] C. Rubbia, J.A. Rubio, S. Buono, F. Carmianti, N. Fìetier, J. Galvez, C. Gelès, Y. Kadi, R. Klapish, P. Mandrillioni, J.P. Revol, C. Roche, European Organisation for Nuclear Research, CERN report AT/95-44 (ET), 1995.
[2] L. Cinotti, M. Bruzzone, S. Cardini, G. Corsini, G. Saccardi, XADS Pb–Bi Cooled Experimental Accelerator Driven System Reference Configuration, Doc. ANSALDO ADS1 SIFX 0500, June 2001.
[3] G.S. Bauer, M. Salvatores, G. Heusener, J. Nucl. Mater. 296 (2001) 17.
[4] H. Aït Abderrahim, P. Kupschus, E. Malambu, Ph. Benoit, K. Van Tichelen, B. Arien, F. Vermeersch, P. D'hondt, Y. Jongen, S. Ternier, D. Vandeplassche, Nucl. Instrum. and Meth. A 463 (2001) 487.
[5] G. Müller, G. Schumacher, F. Zimmermann, J. Nucl. Mater. 278 (2000) 85.

[6] B. Xiaoyi He, N. Li, M. Mineev, J. Nucl. Mater. 297 (2001) 214.
[7] F. Barbier, G. Benamati, C. Fazio, A. Rusanov, J. Nucl. Mater. 295 (2001) 149.
[8] G. Benamati, P. Buttol, V. Imbeni, C. Martini, G. Palombarini, J. Nucl. Mater. 279 (2000) 308.
[9] G. Benamati, P. Buttol, V. Imbeni, C. Martini, G. Poli, Workshop on Heavy Liquid Metal Technology, Karlsruhe, 16–17 September 1999, FZK Report: FZKA 6389, December, 1999.
[10] J.R. Weeks, A.J. Romano, Corrosion – Nace 25 (3) (1969) 131.
[11] O. Kubaschewski, C.B. Alcock, P.J. Spencer, Materials Thermochemistry, 6th Ed., Pergamon, Oxford, 1993.
[12] I. Ricapito, C. Fazio, G. Benamati, J. Nucl. Mater. 301 (2002) 60.
[13] G. Benamati, C. Fazio, I. Ricapito, Mechanical and corrosion behaviour of EUROFER 97 steel exposed to Pb–17Li, 10th International Conference on Fusion Reactor Materials, 14–19 October 2001, Baden-Baden, Germany.
[14] N. Simon, A. Terlain, T. Flament, J. Nucl. Mater. 254 (1998) 185.
[15] G. Ilinecev, REZ doc.: Nr. DITI 11 641 M, July 2001.
[16] G. Benamati, in: Proceeding of the Fifth Workshop on Liquid Metal Blanket Experimental Activities, 16–18 September 1997, Paris, France, CEA report DMT 97/442, SERMA/LCA 2113.
[17] H.U. Borgstedt, H.D. Rohrig, J. Nucl. Mater. 179–181 (1991) 596.
[18] O.K. Chopra, D.L. Smith, J. Nucl. Mater. 141–143 (1986) 566.
[19] H.U. Borgstedt, M. Grundmann, Fusion Eng. Des. 6 (1988) 155.
[20] G. Nicaise, A. Legris, J.B. Vogt, J. Foct, J. Nucl. Mater. 296 (2001) 256.
[21] T. Sample, H. Kolbe, J. Nucl. Mater. 283–287 (2000) 1336.
[22] V. Troyanov, A. Rusanov, IPPE doc. UDC 621.029.553, Obninsk, 2001.
[23] M. Broc, P. Fauvet, T. Flament, A. Terlain, J. Sannier, Proceeding on the Fourth International Conference on Liquid Metal Engineering and Technology, 17–21 October 1988, Avignon, France.
[24] H.U. Borgstedt, Chemische Eigenschaftern des flüssigen Blanketstoffs Pb17Li, FZK report, KfK 4620, August 1989.